IEEE Access
Multidisciplinary | Rapid Review | Open Access Journal

Received August 8, 2017, accepted September 28, 2017, date of publication October 11, 2017, date of current version November 7, 2017.

Digital Object Identifier 10.1109/ACCESS.2017.2761701

Data-Driven Corpus Callosum Parcellation Method Through Diffusion Tensor Imaging

GIOVANA COVER[1], MARIANA PEREIRA[1], MARIANA BENTO[2], SIMONE APPENZELLER[1], AND LETICIA RITTNER[3], (Member, IEEE)

[1]Medical Image Computing Laboratory, School of Electrical and Computer Engineering, University of Campinas, Campinas 13083-852, Brazil
[2]Radiology and Clinical Neuroscience, Hotchkiss Brain Institute, University of Calgary, Calgary, AB T2N 1N4, Canada
[3]Rheumatology Department, Faculty of Medical Science, University of Campinas, São Paulo 13083-970, Brazil

Corresponding author: Giovana Cover (giovanacover@gmail.com)

This work was supported in part by the Coordination for the Improvement of Higher Education Personnel (CAPES) and in part by the São Paulo Research Foundation (FAPESP) under Grant 2013/07559-3.

ABSTRACT The corpus callosum (CC) is a set of neural fibers in the cerebral cortex, responsible for facilitating inter-hemispheric communication. The CC structural characteristics appear as an essential element for studying healthy subjects and patients diagnosed with neurodegenerative diseases. Due to its size, the CC is usually divided into smaller regions, also known as parcellation. Since there are no visible landmarks inside the structure indicating its division, CC parcellation is a challenging task and methods proposed in the literature are geometric or atlas-based. This paper proposed an automatic data-driven CC parcellation method, based on diffusion data extracted from diffusion tensor imaging that uses the Watershed transform. Experiments compared parcellation results of the proposed method with results of three other parcellation methods on a data set containing 150 images. Quantitative comparison using the Dice coefficient showed that the CC parcels given by the proposed method has a mean overlap higher than 0,9 for some parcels and lower than 0,6 for other parcels. Poor overlap results were confirmed by the statistically significant differences obtained for diffusion metrics values in each parcel, when using different parcellation methods. The proposed method was also validated by using the CC tractography and was the only study that proposed a non-geometric approach for the CC parcellation, based only on the diffusion data of each subject analyzed.

INDEX TERMS Diffusion tensor imaging, image processing, image segmentation, magnetic resonance imaging.

I. INTRODUCTION

The corpus callosum (CC), also known as the callosal commissure, with the largest amount of white matter in the brain, is a set of neural fibers in the cerebral cortex, responsible for connecting both brain hemispheres and improving inter-hemispheric communication [1]. The CC has topographic fibers organization related to the brain cortex regions [2].

The CC structural characteristics appear as important elements for studying not only aging, gender differences [3] and laterality [4], but also diseases such as autism [5], depression [6], and obesity [7]. The CC analysis is also recurrent step in neurodegenerative diseases studies, such as Alzheimer's [8], schizophrenia [9], epilepsy [10], dyslexia [11] and multiple sclerosis [12].

Due to its size, the CC is usually divided into smaller regions according to its fibers organization. Each region may be associated with a particular area of the cortex, which is related to specific brain functions. The region containing the CC splenium and body includes fibers of the prefrontal cortex (F) (Fig. 1a). The CC genu is a narrow region including the motor (M), somatosensory (Ss) and auditory (A) cortex. The area between the CC isthmus and the rostrum contains fibers that connect the parietal lobe with the perisylvian zone (P/T), related to language processes. While the CC posterior part is located the rostrum, which contains the fibers of the visual and parietal lobe (V), responsible for the spatial information interpretation [13].

The callosal fibers that interconnect the primary sensorimotor regions (III) are large and strongly myelinated, whereas the callosal fibers that interconnect associative areas are small and not myelinated (I) (Fig. 1b). The highest density of the large fibers is found in the CC body of (III and IV), for the motor, somatosensory and auditory cortices, and CC posterior splenius (V) for the visual cortex. However, the highest

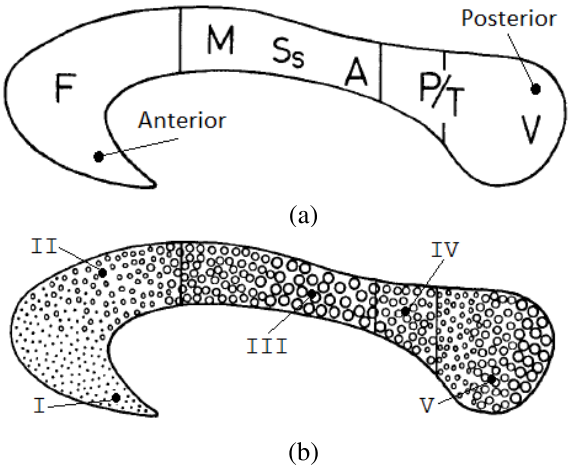

FIGURE 1. CC scheme divisions, identifying different regions for: (a) brain cortical area connections in the anteroposterior direction, with F: frontal, M: motor, Ss: somatosensory, A: auditory, P / T: temporal parietal and V: visual; (b) Distribution of the CC axial fibers according to their diameter: (I) rostrum, (II) genu, (III) body, (IV) isthmus and (V) splenium. Adapted from [13].

fibers density is found in the CC genu and anterior splenius (I, II), associated with temporoparietal and prefrontal brain areas [14].

Between its functions, the CC facilitates interactions for perceptual and cognitive information, being essential for performing visual and tactile tasks. The fibers that cross the CC anterior portion are necessary for the realization of manual movements. While the fibers that cross the CC posterior portion have an important role in the brain visuospatial and visual integration, besides being important in social, attention and emotional functions [14].

This CC subdivision into smaller fractions is called parcellation. As there are no visible landmarks that allow the CC subdivision in the midsagittal plane, geometrical parcellation methods have already been proposed, taking into account *postmortem* analyzes, based on the study of cerebral histology [15]. Subsequently, studies with brain fiber composition analyzed in microscope were done, revealing a pattern capable of differentiating the CC regions [1].

The CC parcellation using medical imaging analysis is also relevant since it is a necessary step to CC area and size studies [3], [16], [17], and because it helps to analyze internal CC properties [18]–[20], as well as human cerebral connectivity [21], [22]. However, existing CC parcellation methods can be classifed as geometric approaches, as they propose the CC parcellation obeying specific proportions, in relation to the CC length, applied in the same way to all dataset, not taking into account the variability among subjects.

One of the most relevant visualization and analysis tool that supports the study of the cerebral anatomy is the Magnetic Resonance Imaging (MRI). It is often used for brain structures analysis, offering a better contrast between soft tissues when compared to other medical images [23]. One modality of MRI is the diffusion tensor imaging (DTI), known to be sensitive to the random motion of water molecules, and being able to quantify the water diffusion in biological tissues [24]. Since the CC presents well-oriented fibers perpendicular to the midsagittal plane, DTI generates good contrast between CC and other cerebral structures [1].

However, automatic image-based CC parcellation is challenging even for specialists since there are no visible landmarks indicating where it should be subdivided. Moreover, since there is no gold standard nor evaluation metrics, it is very difficult to verify the quality of methods already established. and to validate new methods.

TABLE 1. Existing CC parcellation methods.

Modality	[Ref.]	Method	Parcel Number	Subject Quantity
Histological Slide	[15]	Histology	5	15
DTI	[25]	Tractography	6	8
	[26]	Tractography	6	8
	[27]	Tractography	5	8
	[19]	Tractography	6	22
	[28]	Tractography	7	315
	[29]	Watershed	5	15
HARDI	[30]	Tractography	7	20

There are in the literature seven automatic image-based CC parcellation approaches (Table 1), all based on DTI [19], [25]–[30], and one based on a *postmortem* brain study. Six works use the tractography to parcellate, which is a method of representing the fibers of the cerebral cortex trough diffusion data [31]. None of these studies present comparisons between proposed methods or quantitative results.

The objective of this work is to propose an automatic CC parcellation method using diffusion properties extracted from DTI. The CC parcellation proposed is based on the previously developed method by Rittner [29], which uses the Fractional Anisotropy (FA) map and the Watershed transform from markers. Among all seven image-based CC parcellation methods, the Rittner approach was the only study that proposed a non-geometric analysis for the CC parcels, based only on the diffusion data of each subject analyzed. It presented good initial results, however it was tested on a small dataset and was not compared against other methods.

II. CC PARCELLATION METHODS

A geometric CC parcellation method was proposed by Witelson [15], based on *postmortem* connectivity analyses in primates and humans. Though, geometric approaches only divide the CC structure with the same proportion between all subjects, not considering the individual brain characteristics among different subjects.

Huang *et al.* [25] combined the tractography and the cerebral connectivity analysis, using the CC fibers connecting the brain cortex to define CC parcellation regions. Six specific image planes were set as regions of interest (ROI), mapping the fibers that pass through the CC structure, performing the

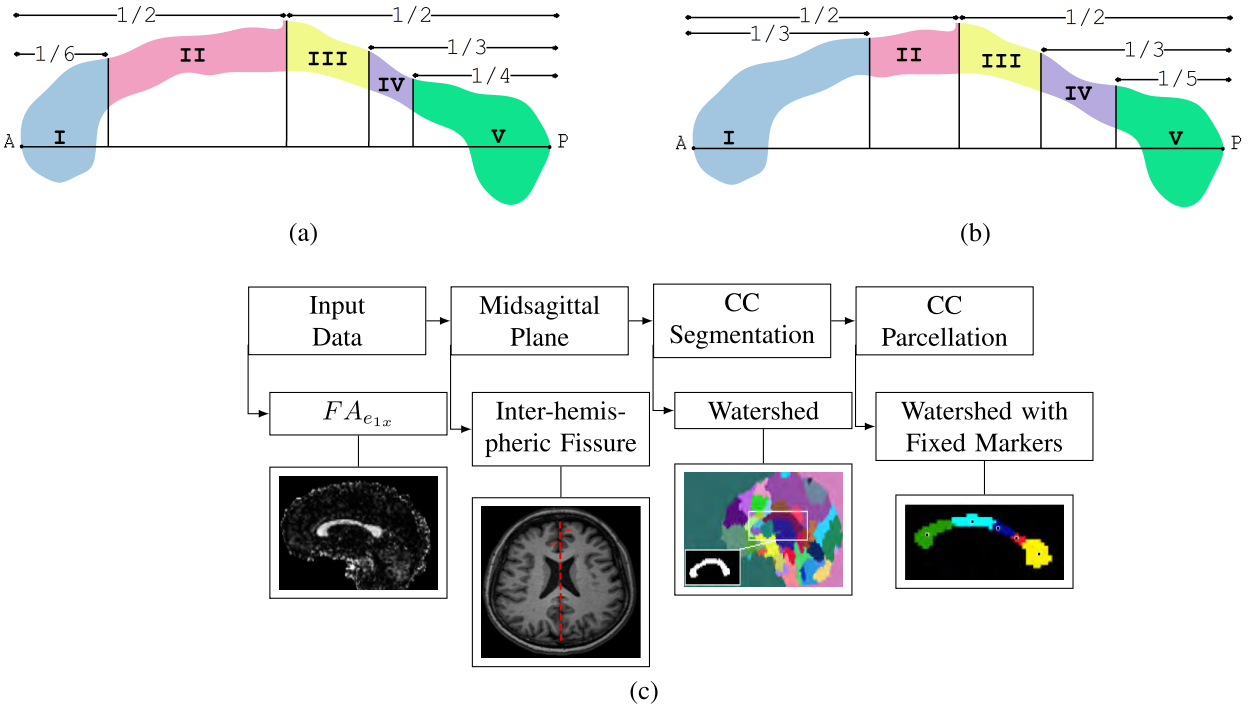

FIGURE 2. **CC parcellation with divisions identifying the resulting five regions: (a) Witelson method; (b) Hofer method; (c) Rittner method, with its four main steps: input data selection, midsagittal slice selection, CC segmentation and final parcellation.**

tractography to determine the fibers crossing each ROI and also the CC section.

Cook [26] proposed a parcellation method with cerebral connectivity in DTI using an atlas segmentation model to label the cortex and find distinct sub-regions in the CC according to their fibers connection. In the work of Park [19], the determination of the ROI for tractography was even more specific, by choosing 47 cerebral cortex sub-regions. However, between DTI studies based on tractography, the CC parcellation performed by Hofer [27] was the only work that proposed a scheme for the CC subdivision from an average behavior observed through tractography in a population. The work proposed by Lebel [28] also used tractography to subdivide the CC into distinct regions, but it is based on target areas for the analysis of aging variation in the cerebral cortex of seven CC regions.

Unlike the CC parcellation methods that use the analysis of the cerebral connectivity by tractography, Rittner [29] proposed a data-driven method, using the specific information contained in the diffusion images of each subject. The CC parcellation method proposed by Rittner was applied in the brain midsagittal plane and performed through the Watershed algorithm, finding five distinct regions. Finally, the work performed by Chao [30] computes the CC parcellation according to the topography of its structure through the connection of the CC fibers made in a probabilistic way. It was based on an analyzed population, using the high angular resolution diffusion images (HARDI), where the anatomical tractography is estimated and incorporated into the final CC parcellation.

We compared our proposed data driven CC parcellation method with the methods proposed by Witelson [15], Hofer [27] and Rittner [29], since they all presented five CC parcels as result, making possible to quantitatively and qualitative compare them.

A. WITELSON PARCELLATION

The Witelson CC parcellation method [15] is based on the brain histological analysis in *postmortem* studies. The Witelson parcellation method proposes to divide the CC into five vertical sections, with borders perpendicular to the axis that connects the CC in horizontal limits, at the anteroposterior section (Fig. 2a).

In this CC parcellation scheme, the region *I* corresponds to the anterior third and contains fibers that are projected in the prefrontal and pre-motor areas of the cortex. The region *II*, composed by the remaining CC anterior half, contains motor fibers. The initial part of the CC posterior half, region *III*, has projections of the somatosensory and posterior parietal areas. While the isthmus, which is equivalent to the region *IV*, has projections of the upper temporal and posterior parietal part. The region *V* corresponds to the projections for the inferior occipital and temporal cortex (Table 2).

However, since it is based entirely on *postmortem* data, dependent on the brain conservation process, the proposed CC parcellation scheme presents some significant differences when anatomically analyzed the structure, not reflecting the internal CC organization [27].

B. HOFER PARCELLATION

The Hofer CC parcellation scheme [27] uses brain connectivity, as tractography, to define all regions connected to distinct brain areas by CC fibers. The geometric parcellation proportion came from the average result analyzed in a study population of 8 subjects. ROI selected using tractography were also chosen in the cortex, representing significant areas connected to the CC structure. Therefore, five vertical sections of the CC were delimited from the tractography study based on all CC connections (Fig. 2b).

The region I, which corresponds to the first sixth, contains fibers projected in the prefrontal region. The remaining CC anterior half, region *II*, contains fibers projecting into the motor-premotor and motor areas of the cerebral cortex. Together, these fibers combine the largest CC region and are located in the back section of the structure. The region III is defined as the posterior half minus the posterior third, containing fibers that are projected in the primary motor cortex. However, this parcellation scheme is in conflict with the Witelson method, which assumes that all primary motor fibers cross the CC anterior half. The region *IV*, the posterior third minus the posterior quarter, refers to the primary sensory fibers. Finally, the parietal, temporal and visual fibers cross the CC region *V*, which is defined as the CC posterior quarter. Unlike the Witelson approach, the Hofer CC parcellation study showed that motor fibers cross the CC structure in the posterior part of the central region (Table 2).

TABLE 2. Anatomical labels attributed to the CC parcellated regions, according to their fibers in relation to the cortical areas as proposed by Witelson and Hofer.

Regions	Witelson Parcellation	Hoffer Parcellation
I	Prefrontal caudal and orbital, lower premotor	Prefrontal
II	Premotor	Premotor, supplemental motor
III	Somatosensory, posterior parietal	Primary motor
IV	Temporal superior, posterior parietal	Primary Sensory
V	Occipital, inferior temporal	Parietal, temporal and visual

C. RITTNER PARCELLATION

Different from other methods, Rittner CC parcellation method [29] takes into account only the input DTI data for the parcellation analysis, using the Watershed algorithm. It is, therefore, a data-driven method, different from geometric parcellation approaches. The method can be described in four steps.

The first step is the weighting of the fractional anisotropy, which is the difference measure between the axes lengths of an ellipsoid [32], by the projection of the eigenvector in the main direction FA_{e_1x}. The second step is the selection of the brain midsagittal plane through the inter-hemispheric fissure, followed by the CC segmentation by Watershed and its parcellation with fixed markers (Fig. 2c).

1) INPUT DATA

Since the CC is a white matter structure with highly organized fibers connecting the two brain hemispheres, it has high FA values, and the diffusion in its fibers occurs mainly in the right-left direction. The FA map is combined with the principal eigenvector component in the right-left direction FA_{e_1x} to emphasize and facilitate the CC segmentation.

After defining the scalar map FA_{e_1x} to the CC segmentation, the external morphological gradient is calculated. Since the CC is a very thin structure, combined with the DTI low resolution, the external gradient highlights the CC edges and helps the Watershed transform segment the desired structure.

2) MIDSAGITTAL PLANE SELECTION

After selecting the input data, the most representative CC central slice is chosen through its diffusion properties by the FA map, taking into account the inter-hemispheric area of the brain. The central portion of the brain is identified by the diffusion properties observed in the inter-hemispheric fissure: large areas corresponding to the cerebrospinal fluid, which has low FA values. Initially, the FA average is calculated for each slice, discarding those slices whose FA average value is above a threshold. The central slice of the brain is the one that has the lowest FA average value, determining the brain midsagittal plane selection.

3) CC SEGMENTATION

The Watershed transform using markers is used to perform the CC segmentation. A hierarchical approach is employed to obtain the most significant regions of the image: the local minimum hierarchy is constructed from the volume dynamics, and the local minimums with higher extinction values are used as markers in the Watershed transform [33]. The number of markers chosen need to be sufficient to capture the edges of the CC. After the Watershed transform is performed, an additional step is needed to automatically cluster the resulting regions, deciding which ones correspond to the CC and which are part of the background. The weighted map average for each of the regions is used to generate the final CC segmentation, since the regions that have a higher average than the others are generally part of the CC.

4) CC PARCELLATION

After segmenting the CC, its parcellation is performed again using the Watershed transform [33]. However, different from the segmentation, fixed markers are positioned along the CC central line as the algorithm markers to perform the final parcellation. The positioning of the Watershed transform markers along the parameterized CC central line were set at the [25, 80, 115, 140, 170] position, based on an analysis of diffusion properties of fifteen subjects along the CC center line.

After the parcellation markers were selected, the method is initialized with the weighted map FA_{e_1x}. The inner edges of the structure are detected by using the morphological gradient

only for the voxels within the CC. The parcellation is found by the Watershed transform, which obtains the final division of the structure.

III. PROPOSED DATA DRIVEN CC PARCELLATION METHOD

We propose a CC parcellation method based on Rittner [29] method, making important changes in order to overcome its limitations and sensitivity to parameters selection. The original method presents four steps described in the last section: input data selection, midsagittal plane selection, CC segmentation and CC parcellation. Almost all steps were replaced with exception of the first step, leading to a more robust and data-driven method.

A. MIDSAGITTAL SLICE SELECTION

The proper analysis of the CC structure in 2D requires the determination of the slice that best defines it [34]–[37]. Rittner's midsagittal plane selection through the inter-hemispheric approach does not take into account the CC specifically, but rather the whole brain. In addition, the inter-hemispheric method ignores cases where the subject's head was misaligned relatively to the MRI acquisition plane.

A method to find a callosal fibers convergence plane (CFCP) was previously proposed [38], taking into account the high organization of the fibers within the CC structure. This plane is computed directly in the diffusion images and specific for 2D CC studies. The CFCP is calculated through divergent maps and finds the plane of greatest convergence of fibers within the structure.

The CFCP computation has three main steps: the automatic identification of the CC, the calculation of the divergent map and the adjustment of the plane (Fig. 3).

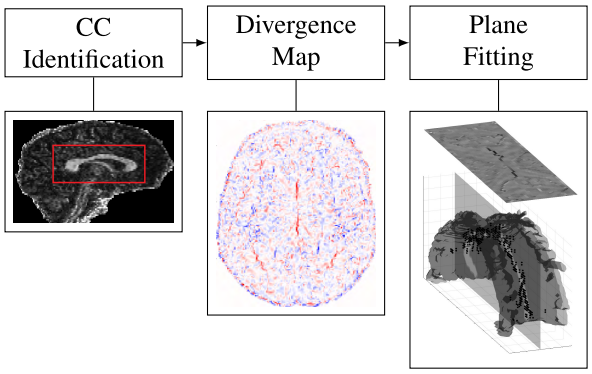

FIGURE 3. Execution steps of the midsagittal slice selection by the callosal convergence plane method.

1) CC IDENTIFICATION

Initially, the CC identification is done through the structure segmentation by using the Watershed transform method [29]. Based on the average point of the segmented CC, a volume of interest of $(36 \times 90 \times 18)$, after interpolation in the z axis, is selected for all subjects. The dimensions of the volume are based on previous knowledge of the CC structure size.

2) DIVERGENCE MAP COMPUTATION

After the identification of the CC structure, the divergent map is computed by converting the DTI tensor field to a vector field oriented in a direction of analysis, as implemented by Pinheiro [39]. The application of the concept of divergence to vectors fields allows the extraction of information about the CC fibers behavior. Positive divergence values are associated with fiber dispersion, while negative values are related to the convergence of the fibers to a point. In addition, parallel fibers tend to have the value of the divergence map close to zero. The CC, due to its shape, has points with maximum absolute divergence located in the maximum convergence plane when the direction of analysis belongs to the CC sagittal plane.

3) PLANE FITTING

In order to establish the plane of maximum convergence of the fiber, which is the CFCP, directions of analysis are applied while searching for a plane in which the vector is perpendicular to these directions.

After converting the data to a vector field-oriented study, calculating the divergence map and excluding points of low diverge values (< 0.4), a single plane is defined, that best describes the remaining points (high diverge values). The plane is computed by using a least square method iteractively, discarding 2% of the points most distant from the calculated plane in each iteration. These steps are performed for a range of temptative directions. Finally, the chosen plane is the one in which the direction of the analysis is closer to being perpendicular to the normal plane vector.

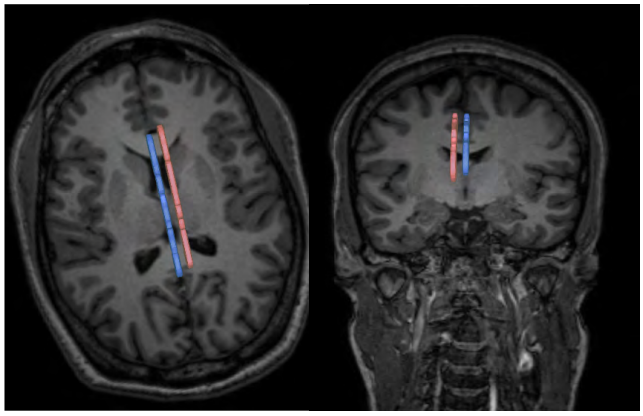

(a) (b)

FIGURE 4. (a) Comparison between the CC midsagittal plane found by the divergent (blue) and inter-hemispheric (red) method for the axial view in T_1; and (b) coronal view in T_1.

When compared to the inter-hemispheric approach, the CFCP may coincide or not (Fig. 4a-b). It depends on weather the CC is misaligned in relation to the acquisition plane or the CC is anatomically aligned with the inter-hemispheric fissure.

B. CC SEGMENTATION

The next step is the CC segmentation. The CC segmentation, as proposed by Rittner, was evaluated in one hundred and fifty subjects. Among these patients, there were ten cases whose segmentation did not work properly including cases in which regions not belonging to the CC were added to the final result and also, cases in which areas belonging to the structure were omitted.

The original CC segmentation is performed by computing an external morphological gradient on the input image to obtain the CC boundaries through the watershed transform from markers. However, in cases where the final CC segmentation failed, it was observed that the morphological gradient had flaws (Fig. 5a).

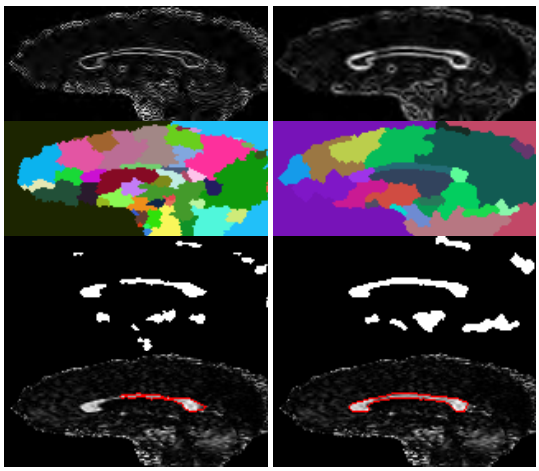

(a) (b)

FIGURE 5. (a) CC segmentation steps by Rittner with the input image morphological gradient, Watershed segmentation markers, remaining FA regions and final segmentation; (b) Result of the proposed CC segmentation, with the addition of a Gaussian filter in the input image morphological gradient.

In order to get better CC boundaries after the external morphological gradient computation, a Gaussian filter was applied to the input image (Fig. 5b). The Gaussian filter emphasizes the CC contours and, consequently, facilitates the final CC segmentation.

C. CC PARCELLATION

The final step, namely the CC parcellation by Watershed, proposed by Rittner, places markers in the same position for all subjects, making it non-specific for each subject (not data-driven). The position of each marker was chosen empirically based on the study of a population constituted of fifteen subjects, being defined as [25, 80, 115, 140, 170] along the CC center line.

In order to generalize the CC parcellation method, a new approach to find individual markers for each subject was proposed. After the CC central line is found (Fig. 6a), a k-means algorithm is used to cluster the two hundred points within this line, based on its FA values. The number of clusters was selected as $k = 5$, since it is the number of the desired CC parcels.

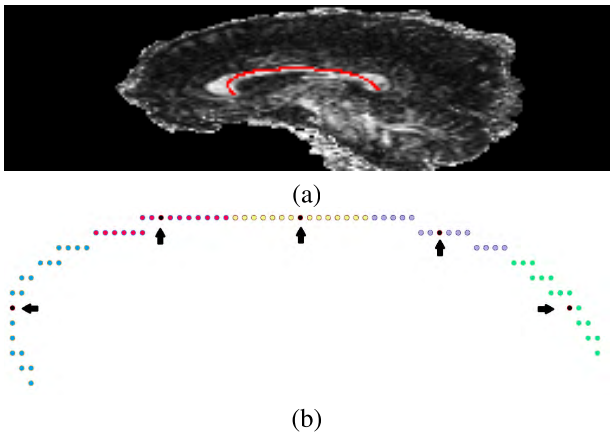

(a)

(b)

FIGURE 6. (a) Brain midsagittal slice with the CC center line in red with FA values used as the k-means algorithm input; (b) k-means output with five clusters and final centroids used as markers to the CC Watershed parcellation.

The k-means algorithm is an unsupervised clustering method, which finds the similarity of a data group and labels them in clusters. It also enables the centroid calculation of each resulting cluster. The points located in the centroids of each parcel resulting from the k-means are then used as the new markers for the Watershed parcellation (Fig. 6b).

IV. QUANTITATIVE AND QUALITATIVE COMPARISON BETWEEN CC PARCELLATION METHODS

We quantitatively and qualitatively compared the proposed parcellation method with related methods presented in the literature. Moreover, first we compared the Rittner approach with the two other methods that divide the CC into five regions: Witelson [15] and Hofer [27]. By doing so, we are able to evaluate if the proposed data-driven CC parcellation method actually improved the results obtained by Rittner.

It is expected that the CC parcels given by Rittner might be closer to the Hofer parcels, than Witelson, since both are based on the CC connectivity with the cortex. The same behavior is expected from the proposed method.

A. DATASET

All methods were evaluated using the same dataset, composed by one hundred and fifty subjects, from the Hospital das ClÃnicas of the State University of Campinas. The dataset was acquired on a Philips Achieva Magnetic Resonance scanner. The images present a slice thickness of $2mm$, resolution of $1mm \times 1mm$, $2mm$ between each slice, dimensions of $(256 \times 256 \times 70)$, interpolated by the MR machine from a image of $(128 \times 128 \times 70)$. The DWI was acquired in 32 spin echo directions DwiSE sequence, with b of $1000s/mm^2$, $TR = 8.5s$, $TE = 61ms$ and one more volume with $b = 0$. All data were processed using the FSL tool [40] correcting eddy currents, registering the DWIs volumes and generating the tensors (eigenvalues and eigenvectors). All subjects were informed in advance and signed a consent term.

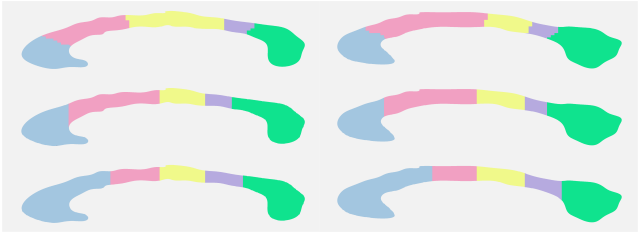

FIGURE 7. CC parcellation result in two distinct subjects (columns) with three distinct parcellation methods (rows): Rittner, Hofer and Witelson.

B. VISUAL COMPARISON

The Rittner CC parcellation method presents an apparent variation in the positioning of the CC parcels for each subject. This happens since this method is only based on the input data and does not follow any atlas or any a priori knowledge (Fig. 7). The same behavior can be observed on the parcellation results from the proposed method (Fig. 8), while both Hofer and Witelson parcellation methods do not change their CC parcels proportion when varying the subjects, since they are geometric approaches.

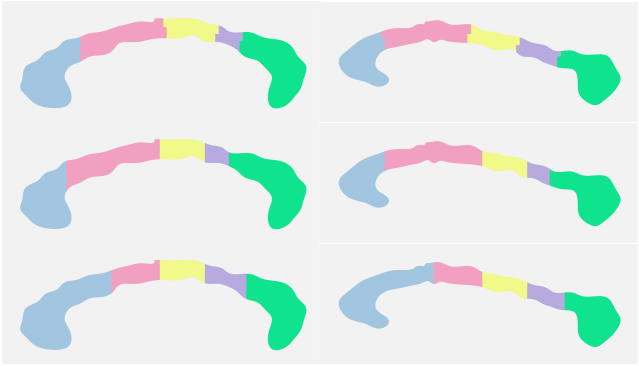

FIGURE 8. CC parcellation result in two distinct subjects (columns) with three distinct parcellation methods (rows): proposed CC parcellation, Hofer and Witelson.

It is also possible to observe that the CC parcellation by the proposed method is similar to the Hofer results as they are based on the connections of the cortical fibers to find the CC parcellation. However, the same does not occur for the Witelson method that is only based on the histological *post-mortem* study. The largest differences between the proposed and Witelson methods are observed in the parcels *I* and *II*.

The similarity between the CC parcellation using the proposed method and the geometric result of Hofer is even more evident when comparing both parcels results (Fig. 9a). It is possible to observe that the CC parcel *IV* from the proposed Watershed method is within the limitations of Hofer's scheme. While the CC parcels *I*, *III* and *IV*, although contained in the delimitations proposed by Hofer, extend to the nearby parcels. The CC parcel *II* is the one that most differs from the geometric approach, being displaced on both sides between distinct subjects. These changes are expected since the proposed CC parcellation by Watershed is data-driven, and generic among subjects.

C. PARCELS OVERLAP

The quantitative comparison between CC parcellation methods was also performed by using an overlap measure, the Dice coefficient [41]. It evaluates the agreement between the results achieved by different CC parcellation methods.

Results showed that the proposed CC parcellation method presented similar Dice coefficient related to the Hofer and Witelson approach on the CC parcels *I* and *III* (Fig. 9b). However, when analyzing CC parcels *II* and *V*, the Dice values obtained for the comparison with the proposed CC parcellation versus the Hoffer parcellation were higher, meaning that they are more similar for these CC parcels. When comparing the proposed CC parcellation to the Rittner's approach, both methods seems very different since Dice coefficients were the lowest among all CC parcels, when compared with other methods.

D. MEAN FA VALUES COMPARISON

A typical clinical study, which uses CC parcellation in DTI, is usually interested in comparing diffusion characteristics, such as FA, between different CC parcels. Thus, the mean FA value of each CC parcel was chosen to study the effect that different parcellation methods might have on FA-based studies.

In order to evaluate the difference in the measured mean FA value from the CC parcels, the analysis of variance (ANOVA) for repeated results was performed, with a complete factorial model, repeated contrast, comparing principal effects through Bonferroni, and measuring p versus the same dependent variable as the evaluated measures [42]. The ANOVA analyzed was implemented using the IBM SPSS Statistics software, available at goo.gl/JTwVbF.

The CC parcellation mean FA results by Rittner have very close median values when compared to the other parcellation methods (Fig. 10a). It is possible to visualize that the CC parcels *III* and *IV* are very similar in all methods. However, when the CC parcels *I*, *II* and *V* are observed, the Witelson method differs from the others, while the Rittner's approach is close to Hofer's CC geometric proportion.

These results were evaluated through the analysis of variance in order to verify if the difference between CC parcels measures are statistically significant. The p values derived from the ANOVA by repetition below 0.05 are considered significant. Results above this threshold are not considered to conclude statistical significance between FA values (Table 3).

The parcels *I* and *V* demonstrated statistical significance in relation to the other parcels. This behavior can be observed in the FA measurements for Rittner parcellation compared to Witelson and Hofer methods.

The comparison of the mean FA values of the parcels obtained by the proposed method with results from Hofer and Witelson, showed that the CC parcel *IV* was the one that presented the most variation between the CC parcellation methods (Fig. 10b). On the other hand, CC parcels *II* and *III* presented the greatest similarity between all methods.

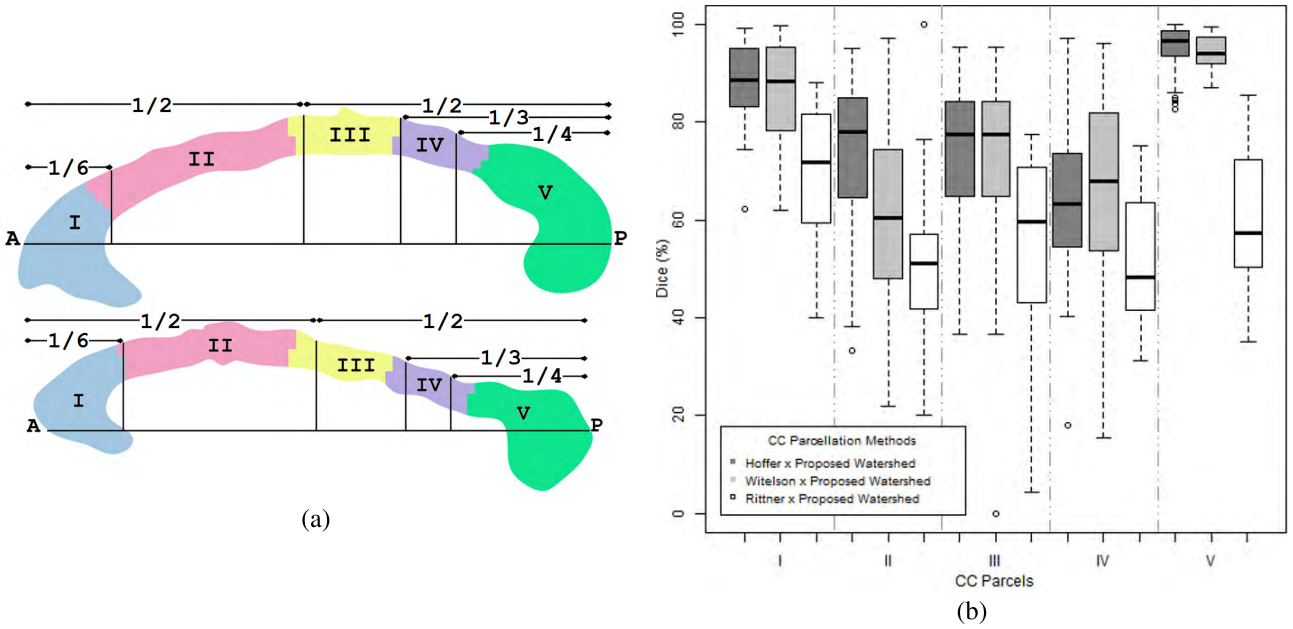

FIGURE 9. Quantitative comparison between CC parcellation methods: (a) Visualization of the proposed CC parcellation in two distinct subjects shown over the geometric proportions defined by Hofer in the anterior-posterior direction; (b) Dice result for each CC parcel, between the proposed and the Hofer, Witelson and Rittner methods.

TABLE 3. ANOVA test by repetition results evaluated for each CC parcel result, with values below $p = 0.05$ considered as statistically significant, among three CC parcellation methods.

Comparison:		Rittner×Witelson	Rittner×Hofer
Measure	**Parcel**	p **value**	p **value**
FA	**I**	**.000**	**.000**
	II	.451	.764
	III	.458	.450
	IV	.597	.059
	V	**.000**	**.000**

TABLE 4. ANOVA test by repetition, among the three CC parcellation approaches: proposed Watershed, Witelson and Hofer methods, evaluated for each CC parcel result.

Comparison:		Proposed Wat.×Witelson	Proposed Wat.×Hofer
Measure	**Parcel**	p **value**	p **value**
FA	**I**	**.000**	.995
	II	.190	.055
	III	.320	.320
	IV	**.001**	**.000**
	V	**.000**	.227

The Witelson approach is the most distinctive method in all CC regions.

For the repeated ANOVA, when inspecting the study between the proposed CC parcellation with the Witelson approach, the parcels *I*, *IV* and *V* showed statistical significance (Table 4). Considering that the Witelson method was based only on the histological brain analysis, while the CC parcellation by Watershed is data driven, such variations are expected.

When analyzing the statistical differences between the proposed CC parcellation and Hofer method, only one CC parcel presented statistical difference between all the analyzed dataset (Fig. 9b). The similarity of the other CC parcel is given because both methods present fundamental similarities: both aim to find the CC parcellation according to its connections, through the callosal fibers to the brain cortex regions. The proportions of the resulting CC parcels, as shown in the qualitative analysis, are visually very similar. However, due to the data driven characteristic that the proposed method has, there is a disagreement between both Watershed and geometric Hofer parcellation for the CC parcel *IV*.

The CC parcel *IV* is the smallest CC region found by the proposed parcellation, and also the smallest portion of the geometric approaches. Thus, the subject variation that only the proposed method has provided presented the statistical significance when compared with the Rittner approach and Hofer geometric CC parcellation.

It is not possible to know the correct CC parcellation since this is a problem without a gold standard. Therefore, the existing analyzes only allow verifying the similarity between the resulting CC parcels, or which present statistical differences between methods of the literature.

Through the qualitative analysis, it is possible to verify the data driven behavior of the proposed method, since the given CC parcels varies according to the subject. The quantitative analysis given by the Dice coefficient showed that the both methods that uses the Watershed transform present different CC parcellation results. Thus, the improvements applied to

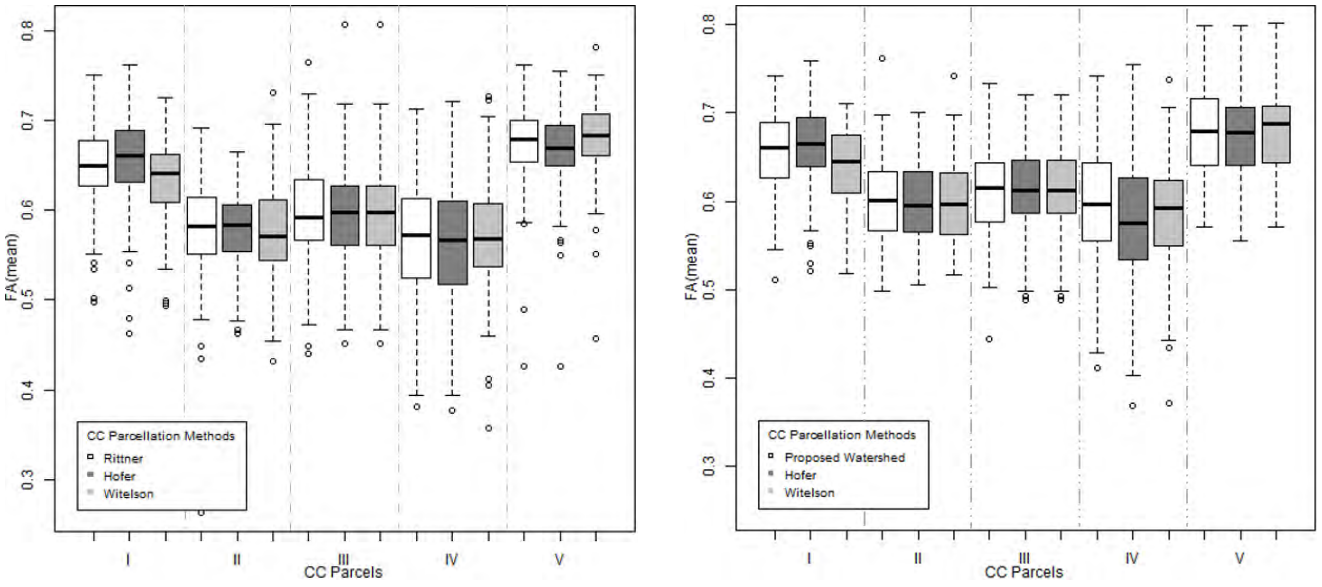

FIGURE 10. Quantitative evaluation by measuring the mean FA for each CC parcel resulted from 150 subjects, between three parcellation methods: (a) Rittner, Hofer and Witelson; (b) Proposed method, Hofer and Witelson. Different values on (a) and (b) for Hofer and Witelson results are due to changes in the midsagittal slice computation and in the CC segmentation step.

the Rittner method in order to make it more robust and less sensitive to parameter selection generated a new method, that presented different results among the experimented 150 subjects, more similar to the Hofer CC parcellation proportion.

E. VISUAL INSPECTION THROUGH TRACTOGRAPHY

In DTI, it was showed that the tensor principal eigenvector is parallel to the white matter fiber local orientation [43]. Using this assumption, the tractography is a method to reconstruct the trajectories of the white matter main fiber bundles through the DTI orientation information, generating three dimensional representations of these bundles. The most recent tractography methods can estimate the regions of multiple fiber bundles [31]. Thus diffusion tensor tractography provides a rough estimate of the location in which the brain fiber bundles cross the cerebral cortex of a subject.

Using the CC parcels obtained by the proposed method as tractography seeds, the tractography was generated using the DSI Studio, a free tractography tool available at http://dsi-studio.labsolver.org/, to design the brain fibers that leave the CC towards the cerebral cortex. It is possible to verify a coherence of the obtained CC parcels by verifying the organization of the fibers coming from the five CC parcels through the tractography (Fig. 11a-c).

Besides coherence verification of the fibers coming from the five CC parcels, the tractography was also used to reconstruct all CC tracks using as seeds the five CC parcels resulted from the proposed data driven parcellation. Then it is possible to verify that each CC parcel is connected to the expected cortical brain region by studying the reconstructed CC tracks. A specialist manually segmented all cortical areas to validate the CC parcel association to distinct brain regions (Fig. 11d-h). Since the parcellation method does not rely on any information from cortical areas, the coherence between them and the resulted CC parcels should be further investigated to verify if this correlation is also statistically observed in a large dataset.

V. DISCUSSION

After quantitatively and qualitatively compare the proposed CC parcellation with the methods proposed by Hofer, and Witelson, it was noted that all CC parcels were distinct among different methods. This conclusion can be particularly confirmed by evaluating the Dice coefficient. If any of the methods were the same, this overlap measurement would have maximum value (equal to one), what was not the achieved result. The most relevant difference between these CC parcellation approaches was related with the data driven behavior presented by the proposed method. While the Hofer and Witelson CC parcellation methods had geometric CC parcels proportion, not varying their results among different subjects throughout the experimented dataset.

Even thought none of the methods presented the same results, some presented interesting similarities. The proposed CC parcellation method was proved to be more closer to the Hofer approach, mainly on CC parcels I, II, III, and V, while the Witelson approach presented significant statistical difference on the CC parcels I, IV and V. When comparing both approaches based on the Watershed transform, our proposed method and the one proposed by Rittner, it was observed that the proposed method presented better generalization capacity and became a fully data driven method, using no fixed markers to run the Watershed transform. The midsagittal plane selection through the callosal plane also

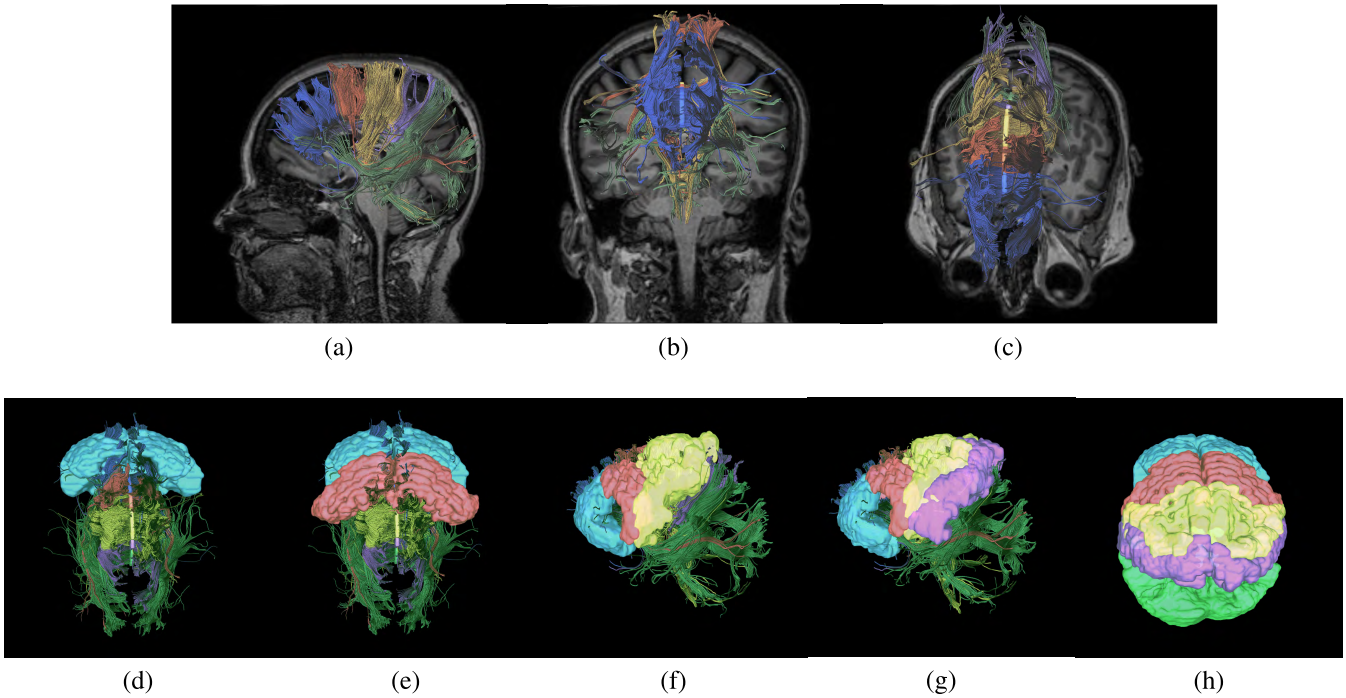

FIGURE 11. Tractography obtained using the resulting parcels as seeds. The five CC parcels are shown in different colors, positioned over T_1 with distinct views: (a) sagittal; (b) coronal; and (c) axial. CC parcellation result along with brain cortical areas referring to the (d) first CC parcel in blue; (e) second CC parcel in red; (f) third CC parcel in yellow; (g) fourth CC parcel in purple; and (h) all CC parcels including the sixth region in green.

improved the method by making it invariant to misaligned CC in relation to the acquisition plane. This improvements were obtained by changing the main steps of the Rittner methods: modifying the brain midsagittal plane selection, the CC segmentation and the CC parcellation. None of the one hundred and fifty subject within the experimented dataset presented errors during the proposed method execution, while the method proposed by Rittner failed in ten subjects during the CC segmentation step.

Since there is no gold standard to evaluate the methods, and considering that all CC parcellation methods presented different approaches and achieved results, we compared the similarities and differences between them. Among the evaluated methods, the proposed one is the only one that is completely data driven and also present no failure while running a large dataset containing 150 subjects. Since brain structures slightly change its size and absolute location among subjects, and that there are lots of applications to study the CC in patients presenting pathologies, a data driven method may be the best automatic CC parcellation solution.

VI. CONCLUSION

Although there are in the literature seven image-based CC parcellation methods, the Rittner approach was the only study that proposed a non-invasive and non-geometric analysis for the CC parcels, based only on the diffusion data of each subject analyzed. The evaluation and improvement of this non-geometric CC parcellation led to the proposal of a new CC parcellation method.

This work proposed an automatic and data-driven method of CC parcellation using diffusion properties extracted from DTI. The improvements made in the original Watershed based method aimed to overcome limitations mainly related with the generalization capacity and parameters sensitivity.

In order to validate the proposed method, it was presented qualitative and quantitative comparisons between the existing CC parcellation methods and the proposed one using statistical analysis of FA mean values and parcels overlap measurements through Dice coefficient.

Quantitative comparisons using the Dice coefficient between the proposed method, Rittner, Witelson and Hofer showed that the CC parcels given by the proposed method are different from the parcels given by Rittner, even though both methods use the Watershed transform. The proposed method presented more similar results with Hofer than the Rittner's.

The proposed method was also validated by using the CC tractography. It verified the coherence of the fibers coming from the five given CC parcels, and that each CC parcel is actually connected to an expected cortical brain region.

REFERENCES

[1] F. Aboitiz, A. Scheibel, R. Fisher, and E. Zaidel, "Fiber composition of the human corpus callosum," *Brain Res.*, vol. 598, no. 1, pp. 143–153, 1992.
[2] K. Rockland and D. Pandya, "Topography of occipital lobe commissural connections in the rhesus monkey," *Brain Res.*, vol. 365, no. 1, pp. 174–178, 1986.
[3] S. C. Johnson, T. Farnworth, J. B. Pinkston, E. D. Bigler, and D. D. Blatter, "Corpus callosum surface area across the human adult life span: Effect of age and gender," *Brain Res. Bull.*, vol. 35, no. 4, pp. 373–377, 1994.
[4] S. F. Witelson and C. H. Goldsmith, "The relationship of hand preference to anatomy of the corpus callosum in men," *Brain Res.*, vol. 545, no. 1, pp. 175–182, 1991.

[5] A. El-Baz *et al.*, "Accurate automated detection of autism related corpus callosum abnormalities," *J. Med. Syst.*, vol. 35, no. 5, pp. 929–939, 2011.
[6] A. L. Lacerda *et al.*, "Anatomical MRI study of corpus callosum in unipolar depression," *J. Psychiatric Res.*, vol. 39, no. 4, pp. 347–354, 2005.
[7] S. Kullmann *et al.*, "Specific white matter tissue microstructure changes associated with obesity," *NeuroImage*, vol. 125, pp. 36–44, Jan. 2016.
[8] N. Rasgon *et al.*, "Agenesis of corpus callosum and dementia of the alzheimer's type: A review and case report," *Can. J. Psychiatry/La Revue Canadienne de Psychiatrie*, vol. 39, no. 7, pp. 429–432, 1994.
[9] S. Bachmann, J. Pantel, A. Flender, C. Bottmer, M. Essig, and J. Schröder, "Corpus callosum in first-episode patients with schizophrenia—A magnetic resonance imaging study," *Psychol. Med.*, vol. 33, no. 6, pp. 1019–1027, 2003.
[10] R. O'Dwyer *et al.*, "Differences in corpus callosum volume and diffusivity between temporal and frontal lobe epilepsy," *Epilepsy Behav.*, vol. 19, no. 3, pp. 376–382, 2010.
[11] K. Von Plessen *et al.*, "Less developed corpus callosum in dyslexic subjects—A structural MRI study," *Neuropsychologia*, vol. 40, no. 7, pp. 1035–1044, 2002.
[12] N. Garg *et al.*, "The corpus callosum in the diagnosis of multiple sclerosis and other CNS demyelinating and inflammatory diseases," *J. Neurol., Neurosurgery Psychiatry*, vol. 86, no. 12, pp. 1374–1382, 2015.
[13] E. Zaidel and M. Iacoboni, *The Parallel Brain: The Cognitive Neuroscience of the Corpus Callosum*. Cambridge, MA, USA: MIT Press, 2003.
[14] T. P. Naidich, M. Castillo, S. Cha, and J. G. Smirniotopoulos, *Imagem do Encéfalo*. Brazil: Elsevier, 2015.
[15] S. F. Witelson, "Hand and sex differences in the isthmus and genu of the human corpus callosum," *Brain*, vol. 112, no. 3, pp. 799–835, 1989.
[16] J. M. Rumsey *et al.*, "Corpus callosum morphology, as measured with MRI, in dyslexic men," *Biol. Psychiatry*, vol. 39, no. 9, pp. 769–775, 1996.
[17] M. Habib, D. Gayraud, A. Oliva, J. Regis, G. Salamon, and R. Khalil, "Effects of handedness and sex on the morphology of the corpus callosum: A study with brain magnetic resonance imaging," *Brain Cognit.*, vol. 16, no. 1, pp. 41–61, 1991.
[18] L. O'Dwyer *et al.*, "Multiple indices of diffusion identifies white matter damage in mild cognitive impairment and Alzheimer's disease," *PLoS ONE*, vol. 6, no. 6, p. e21745, 2011.
[19] H.-J. Park *et al.*, "Corpus callosal connection mapping using cortical gray matter parcellation and DT-MRI," *Human Brain Mapping*, vol. 29, no. 5, pp. 503–516, 2008.
[20] H. D. Rosas *et al.*, "Altered white matter microstructure in the corpus callosum in Huntington's disease: Implications for cortical 'disconnection,'" *NeuroImage*, vol. 49, no. 4, pp. 2995–3004, 2010.
[21] R. F. Dougherty, M. Ben-Shachar, R. Bammer, A. A. Brewer, and B. A. Wandell, "Functional organization of human occipital-callosal fiber tracts," *Proc. Nat. Acad. Sci. USA*, vol. 102, no. 20, pp. 7350–7355, 2005.
[22] M. Wahl *et al.*, "Human motor corpus callosum: Topography, somatotopy, and link between microstructure and function," *J. Neurosci.*, vol. 27, no. 45, pp. 12132–12138, 2007.
[23] R. Edelman and S. Warach, "Magnetic resonance imaging," *New England J. Med.*, vol. 328, no. 10, pp. 708–716, 1993.
[24] R. Bammer, "Basic principles of diffusion-weighted imaging," *Eur. J. Radiol.*, vol. 45, no. 3, pp. 169–184, 2003.
[25] H. Huang *et al.*, "DTI tractography based parcellation of white matter: Application to the mid-sagittal morphology of corpus callosum," *NeuroImage*, vol. 26, no. 1, pp. 195–205, 2005.
[26] P. Cook *et al.*, "An automated approach to connectivity-based partitioning of brain structures," in *Proc. Int. Conf. Med. Image Comput. Comput.-Assist. Intervent.*, 2005, pp. 164–171.
[27] S. Hofer and J. Frahm, "Topography of the human corpus callosum revisited–comprehensive fiber tractography using diffusion tensor magnetic resonance imaging," *NeuroImage*, vol. 32, no. 3, pp. 989–994, 2006.
[28] C. Lebel, S. Caverhill, and C. Beaulieu, "Age-related regional variations of the corpus callosum identified by diffusion tensor tractography," *NeuroImage*, vol. 52, no. 1, pp. 20–31, 2010.
[29] L. Rittner, P. Freitas, S. Appenzeller, and R. Lotufo, "Automatic DTI-based parcellation of the corpus callosum through the watershed transform," *Brazilian J. Biomed. Eng.*, vol. 30, no. 2, pp. 132–143, 2014.
[30] Y. Chao, K. Cho, C. Yeh, K. Chou, J. Chen, and C. Lin, "Probabilistic topography of human corpus callosum using cytoarchitectural parcellation and high angular resolution diffusion imaging tractography," *Human Brain Mapping*, vol. 30, no. 10, pp. 3172–3187, 2009.
[31] A. Alexander *et al.*, "Characterization of Cerebral White Matter Properties Using Quantitative Magnetic Resonance Imaging Stains," *Brain Connectivity*, vol. 1, no. 6, pp. 423–446, 2011.
[32] A. L. Alexander, J. E. Lee, M. Lazar, and A. S. Field, "Diffusion tensor imaging of the brain," *Neurotherapeutics*, vol. 4, no. 3, pp. 316–329, 2007.
[33] J. A. Hartigan and M. A. Wong, "Algorithm as 136: A k-means clustering algorithm," *J. Roy. Statist. Soc. Ser. C (Appl. Statist.)*, vol. 28, no. 1, pp. 100–108, 1979.
[34] B. A. Ardekani, J. Kershaw, M. Braun, and I. Kanuo, "Automatic detection of the mid-sagittal plane in 3-D brain images," *IEEE Trans. Med. Imag.*, vol. 16, no. 6, pp. 947–952, Dec. 1997.
[35] F. P. Bergo, A. X. Falcão, C. L. Yasuda, and G. C. Ruppert, "Fast, accurate and precise mid-sagittal plane location in 3D MR images of the brain," in *Biomedical Engineering Systems and Technologies*. Berlin, Germany: Springer, 2009, pp. 278–290.
[36] Q. Hu and W. L. Nowinski, "A rapid algorithm for robust and automatic extraction of the midsagittal plane of the human cerebrum from neuroimages based on local symmetry and outlier removal," *NeuroImage*, vol. 20, no. 4, pp. 2153–2165, 2003.
[37] Y. Liu, R. T. Collins, and W. E. Rothfus, "Robust midsagittal plane extraction from normal and pathological 3-D neuroradiology images," *IEEE Trans. Med. Imag.*, vol. 20, no. 3, pp. 175–192, Mar. 2001.
[38] G. R. Pinheiro, "Computation of curl and divergence maps from diffusion tensor images and application examples," M.S. thesis, Dept. Elect. Eng, Univ. Campinas, Campinas, Brazil, 2017.
[39] G. R. Pinheiro, G. S. Soares, A. L. Costa, R. A. Lotufo, and L. Rittner, "Divergence map from diffusion tensor imaging: Concepts and application to corpus callosum," in *Proc. 38th Annu. Int. Conf. Eng. Med. Biol. Soc. (EMBC)*, Aug. 2016, pp. 1120–1123.
[40] M. Jenkinson, C. F. Beckmann, T. E. Behrens, M. W. Woolrich, and S. M. Smith, "FSL," *NeuroImage*, vol. 62, no. 2, pp. 782–790, 2012.
[41] L. R. Dice, "Measures of the amount of ecologic association between species," *Ecology*, vol. 26, no. 3, pp. 297–302, 1945.
[42] R. O'Brien and M. Kaiser, "MANOVA method for analyzing repeated measures designs: An extensive primer," *Psychol. Bull.*, vol. 97, no. 2, p. 316, 1985.
[43] P. J. Basser, J. Mattiello, and D. LeBihan, "MR diffusion tensor spectroscopy and imaging," *Biophys. J.*, vol. 66, no. 1, pp. 259–267, 1994.

GIOVANA COVER received the B.S. degree in electrical engineering from the University of Passo Fundo, Passo Fundo, Brazil, in 2015, with an undergraduate exchange program with the Rose-Hulman Institute of Technology, and the M.S. degree in electrical engineering from the University of Campinas, Campinas, Brazil, in 2017. Her research interest includes medical image processing, focusing on magnetic resonance image, brain structure segmentation, and neural networks.

MARIANA PEREIRA received the degree in telecommunication engineering from the Federal University of São João del-Rei in 2016, with an undergraduate exchange program at the University of Alabama at Birmingham. She is currently pursuing the M.Sc. degree in electrical and computer engineering with the University of Campinas. She was an Intern with the Illinois Institute of Technology in 2015. Her research focus is medical image processing, deep learning, and magnetic resonance imaging. She is also interested in neurodegenerative diseases.

MARIANA BENTO received the bachelor's degree (Hons.) from the Federal University of Ceará in 2011, the master's degree with an internship at the Faculty of Electrical and Computer Engineering, University of Pennsylvania, in 2013, and the Ph.D. degree from the Faculty of Electrical and Computer Engineering, University of Campinas, in 2016. She is currently pursuing the Post-Doctoral degree in radiology and clinical neuroscience with the University of Calgary. She was an Intern with the University of Calgary. Her research focus is medical image processing, pattern recognition, and automatic segmentation techniques. Her other applications of interest are texture analysis and brain abnormalities.

SIMONE APPENZELLER received the M.D. and Ph.D. degrees from the Faculty of Medical Science, State University of Campinas. She held a post-doctoral position at McGill University, Canada, and the Stavanger Hospital, Norway. She is currently an Associate Professor with the Rheumatology Department, Faculty of Medical Science, State University of Campinas. Her research is focused on neurologic manifestations and neuroimaging in rheumatic diseases.

LETICIA RITTNER received the degree in electrical engineering, and the M.Sc. and Ph.D. degrees from the University of Campinas, in 1994, 2004, and 2009, respectively, with a six-month internship at the Montreal Neurological Institute, McGill University, Canada. She held a post-doctoral position at the School of Medicine, University of Pennsylvania, in 2012. She is currently an Assistant Professor with the School of Electrical and Computer Engineering, University of Campinas, Brazil. She is also part of the Brazilian Institute of Neuroscience and Neurotechnology. Her research field is medical image processing and analysis, focused particularly on magnetic resonance imaging of the brain.